Fluid flow paths in the Middle America Trench and Costa Rica margin

Eli Silver Earth Sciences Department, University of California, Santa Cruz, California 95064, USA
Miriam Kastner Scripps Institution of Oceanography, La Jolla, California 92093, USA
Andrew Fisher Earth Sciences Department, University of California, Santa Cruz, California 95064, USA
Julie Morris Department of Earth and Planetary Sciences, Washington University, St. Louis, Missouri 63130, USA
Kirk McIntosh Institute for Geophysics, University of Texas, Austin, Texas 78759-8500, USA
Demian Saffer Earth Sciences Department, University of California, Santa Cruz, California 95064, USA

ABSTRACT

The hydrology of the subducting plate and its dewatering behavior through the shallow subduction zone is linked to the structure and deformation of the forearc prism, the nature of the seismogenic zone, the composition of seawater for selected elements, and the composition of the residual slab subducted to depths of magma generation at the volcanic arc. Two locally independent systems of fluid flow govern the transport of heat and chemistry through the Costa Rica subduction complex, a dominantly nonaccretionary subduction zone. One fluid system is the margin wedge, décollement, and underthrust sediment section. Fluid sources include local sediment compaction and mineral dehydration at depth. A second flow system occurs in basement, beneath the sedimentary sequence on the incoming plate. This region is characterized by extremely low conductive heat flow, and the sediment overlying basement has pore-water geochemistry similar to that of seawater. Flow nearly parallel to the trench could be directed by permeability associated with faults and driven by a combination of differential heating and earthquake strain cycling.

Keywords: Central America, geochemistry, heat flow, hydrogeology, subduction zones.

INTRODUCTION

Studies of fluid flow in convergent margins have focused mainly on accretionary systems, such as Barbados, Cascadia, and Nankai (Moore, 1989; Moore and Vrolijk, 1992; Fisher and Hounslow, 1990; Moore et al., 1990; Le Pichon et al., 1992). Here we report on the flow system in a dominantly nonaccretionary subduction zone, located off the Pacific coast of northern Costa Rica (Fig. 1). Nonaccretionary subduction zones have greater opportunity to tap the fundamental fluid pathways coming from deep within the system (Fryer, 1996). These zones show much greater dewatering of subducted sediments, because accretionary systems lose much of their initial water through frontal accretion. Consequently, compositions of fluids sampled in Costa Rica, and their fluxes, may be useful for sampling deeper level processes, including the mineralogical controls on the updip limit of interplate seismicity, the contribution of expelled pore fluids to seawater chemistry, and the effects of such shallow dewatering on the composition of the residual slab subducted to the depths of magma generation.

The margin wedge off northern Costa Rica consists of a relatively high seismic-velocity basement underlying a sedimentary apron, and ending at a small deformed sedimentary wedge at the toe of the margin (Shipley et al., 1992; Christeson et al., 1999). The small deformed wedge (Fig. 2) is lithologically and chemically similar to the sedimentary apron where drilled, not to the incoming sediment section (Kimura et al., 1997). Wedge sediments have extremely low ^{10}Be when compared to the uppermost part of the incoming sediment column (100×10^6 a g^{-1} [atoms per gram] vs. 3000×10^6 a g^{-1}), suggesting that the prism is composed of old material (Valentine et al., 1997). Locally small packages of subcreted strata are imaged in seismic data (Shipley et al., 1992; McIntosh and Sen, 2000), but the bulk of the basement and prism material has too high a velocity to be considered a young accretionary feature, and the margin is dominantly nonaccretionary.

The new seafloor magnetic map (Meschede et al., 1998) shows the primary structural grain of the oceanic crust (Fig. 1) and suggests possible flow pathways. The anomalies are parallel to the trench (generated at the East Pacific Rise) in the Leg 170 area and perpendicular to the trench (generated at the Galápagos spreading center) less than 20 km to the southeast. The boundary between these two zones is called the rough-smooth boundary (RSB), because of the greater seafloor roughness of Galápagos crust than East Pacific Rise crust. The boundary may actually be closer to the drilling transect, because the chemistry of sills encountered beneath the sedimentary sequence were similar to Galápagos rather than East Pacific Rise sources (Kimura et al., 1997). It is possible that the RSB acts as either a source or sink for fluids in the basement.

Five sites were drilled in this area on Ocean Drilling Program Leg 170 (Kimura et al., 1997). Site 1039 was drilled in the trench axis, through 400 m of hemipelagic and pelagic sediment, and bottomed in a set of gabbro sills that have geochemistry similar to rocks at the Galápagos spreading center. This result was unexpected because the sites appear to be on crust generated at the East Pacific Rise (Fig. 1). The oldest sediment above the sill sequence was dated paleontologically as 16.5 Ma, whereas recent seafloor magnetic interpretations give a plate age of 24 Ma (Meschede et al., 1998). Sites 1040 and 1043 penetrated a deformed sedimentary wedge, similar in composition to the slope apron drilled at Site 1041. Both penetrated the décollement and the increasingly dewatered underthrust sequence below. Site 1040 also bottomed in a gabbro sill. Site 1041 penetrated most of the sedimentary apron that is above high-velocity prism material. Site 1042 sampled the upper 60 m of the prism beneath the apron, retrieving clasts of sandstone breccia, chert, and basalt with affinities to onland exposures, but not to the incoming sediment section as seen at Site 1039 (Kimura et al., 1997). Heat flow was measured at Sites 1039, 1040, and 1041.

FLUID FLOW PATHWAYS IN THE WEDGE AND UNDERTHRUST SEDIMENTS

The pathways of fluid flow through the Costa Rica margin are constrained largely by measured ranges of permeability (Saffer et al., 2000) and pore-water geochemistry. The décollement is one major pathway (Kimura et al., 1997), along which pore-water geochemistry shows low values of chlorinity (Fig. 3D) and salinity and anomalous concentrations and isotope ratios of several components (i.e., Ca [Fig. 3A], Mg [Fig. 3B], Sr, Li, Na, K, Si, ^{87}Sr/^{86}Sr, ^{6}Li/^{7}Li) relative to the pore fluids above and below it. These geochemical indicators most likely result from hydrous mineral

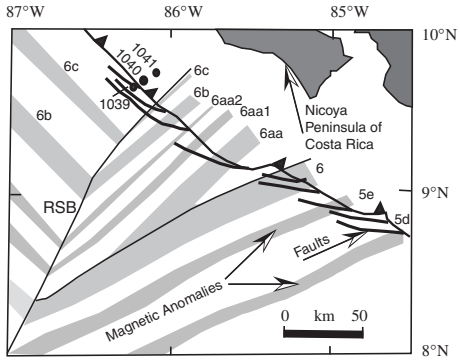

Figure 1. Location of southern Middle America off Costa Rica, showing magnetic anomalies (Meschede et al., 1998), Ocean Drilling Program Sites 1039, 1040, and 1041, and rough-smooth boundary (RSB). Site 1043 is located very close to 1040. Also mapped are deformation front (teeth on upper plate) and faults on oceanic plate in trench.

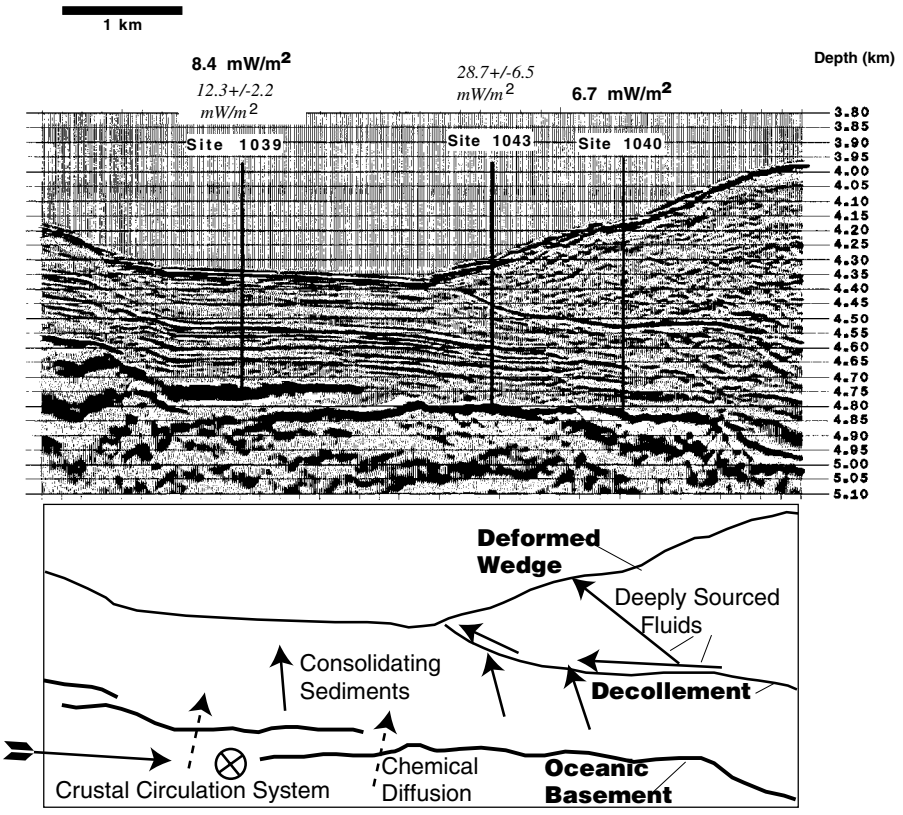

Figure 2. Seismic profile CR20, showing rapid decrease in thickness of underthrust sediment with depth. Profile goes through Ocean Drilling Program Sites 1039, 1043, and 1040 (located in Fig. 1). Numbers at top are mean values of borehole (bold) and surface (italics) heat flow: former are known for Sites 1039 and 1040, latter for 1039 and 1043. Lower diagram shows schematically expected fluid advection (solid arrows) and chemical diffusion (dashed arrows) gradients expected in this system. Circle with x indicates flow out of plane of section.

dehydration and phase transformation at depth. Similar low salinity and chlorinity zones occur within the deformed wedge, as sharp spikes associated with local faults (Fig. 3D). In addition, both the deformed wedge and the sedimentary apron have significantly lower values of salinity and chlorinity than that of reference Site 1039, likely due to mineral dehydration at depth and some in situ gas hydrate decomposition.

The source depths for pore fluids recovered along the décollement can be constrained by fluid geochemistry. Potassium and lithium concentrations and polymerized hydrocarbons in these pore fluids indicate that the mineral dehydration and transformation reaction temperatures are at least 80–120 °C and less than 150 °C (Kimura et al., 1997; Chan and Kastner, 1998). The measured heat flow at Site 1041 is 18 mW/m^2 and the thermal conductivity of the uppermost sediments is ~1 W/mK (Kimura et al., 1997). The seismic velocity in rocks beneath the sediment apron is two to three times that of the apron sediments (Christeson et al., 1999), so we can conservatively consider the thermal conductivity of the deeper rocks to be at least twice that of the sediments. Extrapolating a deep geothermal gradient of about 10 °C/km, temperatures exceeding 100 °C and less than 150 °C would be expected to occur between 10 and 15 km depth.

Loading of the underthrust sediment by the margin wedge generates significant fluid flow by compaction (Kimura et al., 1997; Saffer et al., 2000). Consolidation tests suggest that overpressures in the underthrust sediments increase downsection (Saffer et al., 2000), implying that there is little to no fluid flow downward from the overpressured, dewatering underthrust sediments into upper oceanic basement. That the measured heat flow (discussed in the following) is only 10% of the expected conductive value implies that lithospheric heat is being removed advectively, possibly by lateral flow and subsequent discharge of fluids in basement (e.g., Langseth and Herman, 1981; Langseth and Silver, 1996). The overpressure in the (deformable) sediments just above (presumably much more rigid) basement (~3 MPa above hydrostatic) argues that the fluid in the basement is hydrologically distinct from that in the wedge.

EVIDENCE FOR FLUID FLOW IN BASEMENT

Surface heat-flow observations (Langseth and Silver, 1996) show very low values over the Cocos plate as it enters the subduction zone (8–13 mW/m^2, Fig. 2). These values are well below those expected for 24 Ma crust, 95–105 mW/m^2 (Stein and Stein, 1994). Borehole temperatures (Fig. 3E) and detailed measurements of thermal conductivity support the low surface heat flow values over the Cocos plate and are at the low end (8 mW/m^2) of those observations (Kimura et al., 1997). Rapid flow and replenishment of fluid in basement is indicated by the reversal of pore-water concentration and isotopic gradients in the basal section of the overlying sediment. Near basement the concentration and isotope ratios approach modern-day seawater values. This is most clearly manifested in Ca (Fig. 3A), Mg (Fig. 3B), Sr, Li, and silica concentrations, and Sr (Fig. 3C) and Li isotope ratio depth profiles.

Under diffusive conditions and where young seawater is not present, Ca concentrations increase or remain constant with depth, Mg and Li concentrations decrease, and Si concentrations increase because of diagenetic reactions in hemipelagic and siliceous-calcareous sediments (i.e., McDuff, 1981; Baker et al., 1982). When sediments become enriched in volcanic ash with depth, Ca concentrations in pore waters increase, as at Ocean Drilling Program (ODP) Site 1039 (Fig. 3A). However, in the basal calcareous and volcanic-rich sediments at this site, all these components display concentration reversals near basement (Fig. 3A). The reversal in Mg concentration at about 120 m in Site 1039 (Fig. 3B) is particularly noticeable because in normal oceanic sequences Mg concentrations decrease during seawater-sediment or basalt-seawater interactions at all temperatures (i.e., Mottl and Wheat, 1994). Sr concentrations and Sr isotope ratios, which are strongly affected by diagenetic reactions, also tend to depart considerably from seawater values with depth in most marine sediments, especially in calcareous volcanic-rich sediments (i.e., Baker et al., 1982). Pore-water profiles typically show that dissolved Sr isotope ratios will become either less or more radiogenic through mixing seawater Sr with volcanic ash or detrital clay Sr, respectively. In contrast, Site 1039 Sr concentrations and isotopic values become more radiogenic in a volcanic-rich section (Fig. 3C).

We made preliminary estimates of residence time in the basement fluid flow regime. The estimates are based on the observed chemical and isotopic gradients, the calculated diffusive fluxes from the pore-water values at ~270 m below seafloor to the near basement values, and the time required to evolve modern seawater to the observed altered (near seawater) composition. Calculations of residence time of the basement formation water require a sedimentary diffusion coefficient, which is approximated by dividing the coefficient of molecular diffusion by the product of porosity times formation fac-

tor (Li and Gregory, 1974), both of which are measured on the cores. A sediment diffusion coefficient of 4×10^{-6} cm^2s^{-1} was used for this basal sediment section. On the basis of data from nearby Site 504 and other areas where young basement has been drilled, we assumed that the uppermost 200 m of basement is most permeable and has an effective porosity of 10% (Becker et al., 1989; Fisher, 1998; Becker and Fisher, 2000). For Sr concentration and isotopic ratio gradients in the basal section, this method indicates that the basement formation water is younger than 20 ka. A similar calculation based on dissolved Li and its isotope ratios provides an age younger than 15 ka.

MECHANISMS OF RAPID LATERAL FLUID FLOW IN BASEMENT

The lateral flow of crustal fluids within the Cocos plate at rates sufficient to explain thermal and chemical observations constrains a combination of driving forces and crustal hydrologic properties. One possible driving force is the difference between pressures at the base of cold and warm columns of crustal fluids, at sites of recharge and discharge, respectively. We use calculated pressure differences based on this density contrast to estimate available driving forces and crustal properties, using an analytical thermal model for laterally flowing fluids in upper basement (Langseth and Herman, 1981; Fisher and Becker, 2000). This model accounts for the observed suppression of seafloor heat flow by fluid flowing laterally in uppermost basement between recharge and discharge sites separated by several kilometers or more, assuming that fluid recharge and discharge are rapid and adiabatic. Given a typical sediment thickness of 500 m overlying basement, conductive conditions within the sediments, and seafloor heat flow of 12 mW/m^2, the temperature at the sediment-basement interface would be 52 °C greater than that of bottom water.

If we assume that fluids within a permeable basement layer immediately below the sediments are well mixed and isothermal, and that bottom water is at 0 °C, then the available driving force is: $\Delta P = (\rho_{0°} - \rho_{52°})gh$, where h is the thickness of the sediments (h_s) plus the thickness of the permeable basement layer (h_b). We calculate the specific discharge (volume flux per area) as a function of the thickness of the permeable basement layer and the spacing between recharge and discharge sites (Δx) so that the heat flow halfway between these sites is equal to that observed (12% of the lithospheric value for 24 Ma crust; Fig. 4). Calculated pressure differences vary from 80 to 230 kPa, and bulk permeabilities vary from 10^{-9} to 10^{-14} m^2 (Fig. 4), a range consistent with the global data set of in situ measurements of generally younger crust (Fisher, 1998; Becker and Fisher, 2000). If the pressure difference available to drive flow between recharge and discharge sites is lower, because some head is lost during vertical flow or because temperature differences are less than assumed here, then the associated crustal permeabilities must be greater.

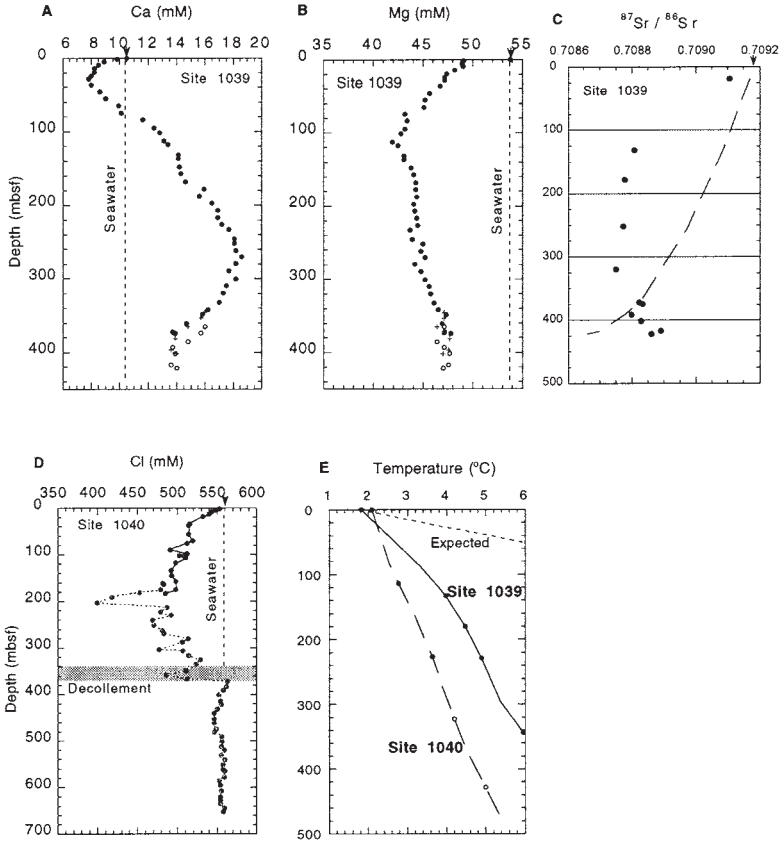

Figure 3. Distributions of pore-water chemistry and temperature vs. depth. A: Site 1039: calcium. Thin dashed line shows seawater values. B: Site 1039, magnesium. C: Site 1039, strontium isotope (dashed line is seawater Sr isotope age trend). D: Site 1040, chlorinity. E: Temperature at Sites 1039 and 1040. Thin dashed line shows expected values for crust of 24 Ma. In all figures, depth is given in meters below seafloor (mbsf) and arrows at top of figures show seawater values.

We use the range of specific discharge values and Figure 4 to compute the residence time of basement formation water to compare with values obtained from geochemistry. Extreme end members are found using the lowest and highest values from Figure 4. Assuming a minimum horizontal flow distance of 2000 m and a permeable basement thickness of 100 m gives a specific discharge of 1 m/yr and thus a minimum residence time of 2000 yr. At the other extreme, a horizontal distance of 80 000 m and a thickness of 1000 m yields a specific discharge of 5 m/yr and a maximum residence time of 16 k.y. These numbers just overlap the range of geochemically determined times of 15 and 20 k.y.

Upper crustal permeabilities could be somewhat lower than indicated by these calculations if additional forces are available to drive lateral fluid flow within oceanic basement. An additional mechanism that may help to drive flow is cyclic seismic flexure and associated crack dilation and contraction (Sibson, 1994; Muir Wood, 1994). Normal faulting in the trench associated with plate flexure will increase crack development during interseismic periods, when crack dilation may allow entrance of fluids into the uppermost crustal rocks, especially where those rocks are exposed to seawater. During coseismic movements fluids could be squeezed out of the newly formed cracks. Regions of locally high permeability could allow enhanced fluid circulation. The magnitude of such flow, however, is unknown. If strain cycling is important for fluid flow in this setting, then the observed heat-flow depression could be a common feature of sediment-poor trenches, e.g., offshore Peru (Yamano and Uyeda, 1990).

CONCLUSIONS

Rapid dewatering of underthrust sediments beneath the deformed frontal sediment wedge probably occurs through narrow, high-permeability zones and may connect with thin vertical conduits. Fluids moving along the décollement originated at ~150 °C, indicating maximum depths between 10 and 15 km, and distances to 40–60 km landward of the trench. Geochemistry and

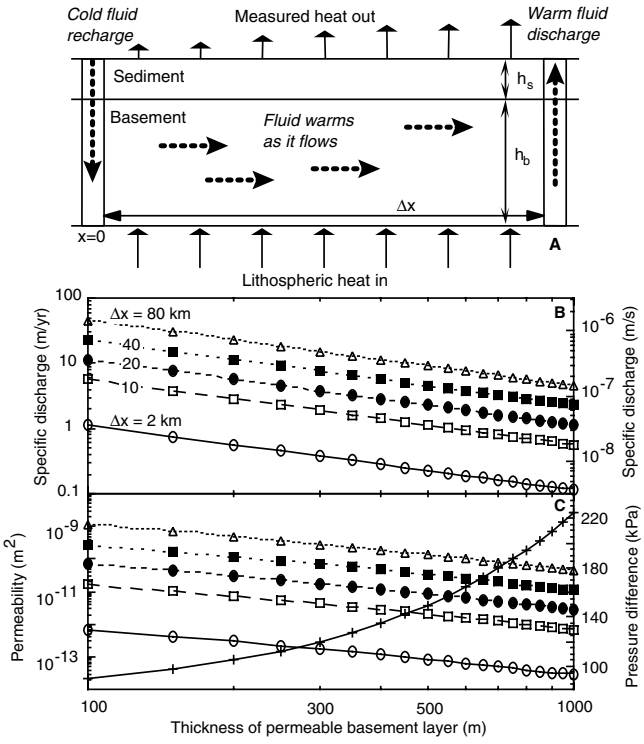

Figure 4. Upper diagram is of temperature-driven fluid circulation model. Lower diagram is plot of specific discharge, permeability, and pressure difference vs. thickness of permeable basement layer, shown for different values of recharge-discharge distance. Solid curve in lower diagram is pressure difference.

both surface and borehole heat flow demonstrate the likelihood of rapid flow of seawater into the uppermost oceanic basement of the Cocos plate at the trench (Fig. 2, lower). Geochemical profiles trend toward seawater values near basement in ODP Site 1039, and heat flow is ~10% or less of that expected for equilibrium conditions. An analytical model shows how temperature differences could drive lateral fluid flow in basement. Driving pressures may be enhanced by crack dilation and contraction through seismic cycles near the trench axis.

ACKNOWLEDGMENTS

Funded by grants from the National Science Foundation and the United States Science Support Program. We thank the Leg 170 participants for their support and Casey Moore and Liz Screaton for very helpful reviews.

REFERENCES CITED

Baker, P.A., Gieskes, J.M., and Elderfield, H., 1982, Diagenesis of carbonates in deep-sea sediments—Evidence from Sr/Ca ratios and interstitial dissolved Sr^{2+} data: Journal of Sedimentary Petrology, v. 52, p. 71–82.

Becker, K., and Fisher, A.T., 2000, Permeability of upper oceanic basement on the eastern flank of the Endeavor Ridge determined with drill-string packer measurements: Journal of Geophysical Research, v. 105, p. 897–912.

Becker, K., Sakai, H., Adamson, A.C., Alexandrovich, J., Alt, J.C., Anderson, R.N., Bideau, D., Gable, R., Herzig, P.M., Houghton, S.D., Ishizuka, H., Kawahata, H., Kinoshita, H., Langseth, M.G., Lovell, M.A., Malpas, J., Masuda, H., Merrill, R.B., Morin, R.H., Mottl, M.J., Pariso, J.E., Pezard, P.A., Phillips, J.D., Sparks, J.W., and Uhlig, S., 1989, Drilling deep into young oceanic crust at Hole 504B Costa Rica Rift: Reviews of Geophysics, v. 27, p. 79–102.

Chan, L.-H., and Kastner, M., 1998, Lithium isotopic composition of fluids and sediments at the Costa Rica subduction zone: Results from ODP Sites 1039 and 1040: Eos (Transactions, American Geophysical Union), v. 79, p. 395.

Christeson, G.L., McIntosh, K.D., Shipley, T.H., Flueh, E., and Goedde, H., 1999, Structure of the Costa Rica convergent margin, offshore Nicoya peninsula: Journal of Geophysical Research, v. 104, p. 25,443–25,468.

Fisher, A.T., 1998, Permeability within basaltic oceanic crust: Reviews of Geophysics, v. 36, p. 143–182.

Fisher, A.T., and Becker, K., 2000, Reconciling heat flow and permeability data with a model of channelized flow in oceanic crust: Nature, v. 403, p. 71–74.

Fisher, A.T., and Hounslow, M.W., 1990, Transient fluid flow through the toe of the Barbados accretionary complex: Constraints from ODP Leg 110 heat flow studies and simple models: Journal of Geophysical Research, v. 95, p. 8845–8858.

Fryer, P., 1996, Evolution of the Mariana convergent plate margin system: Reviews of Geophysics, v. 34, p. 89–125.

Kimura, G., Silver, E.A., Blum, P., et al., 1997, Proceedings of the Ocean Drilling Program, Initial reports, Volume 170: College Station, Texas, Ocean Drilling Program, 458 p.

Langseth, M.G., and Herman, B.J., 1981, Heat transfer in the oceanic crust of the Brazil basin: Journal of Geophysical Research, v. 86, p. 10,805–10,819.

Langseth, M.G., and Silver, E.A., 1996, The Nicoya convergent margin—A region of exceptionally low heat flow: Geophysical Research Letters, v. 23, p. 891–894.

Le Pichon, X., Kobayashi, K., and Kaiko-Nankai Scientific Crew, 1992, Fluid venting activity within the eastern Nankai Trough accretionary wedge: A summary of the 1989 Kaiko-Nankai results: Earth and Planetary Science Letters, v. 109, p. 303–318.

Li, Y.H., and Gregory, S., 1974, Diffusion of ions in seawater and in deep-sea sediments: Geochimica et Cosmochimica Acta, v. 38, p. 703–714.

McDuff, R.E., 1981, Major cation gradients in DSDP interstitial waters: The role of diffusive exchange between seawater and upper oceanic crust: Geochimica et Cosmochimica Acta, v. 45, p. 1705–1713.

McIntosh, K.D., and Sen, M.K., 2000, Geophysical evidence for dewatering and deformation processes in the ODP Leg 170 area offshore Costa Rica: Earth and Planetary Science Letters, v. 178, p. 125–138.

Meschede, M., Barckhausen, U., and Worm, H., 1998, Extinct spreading on the Cocos Ridge: Terra Nova, v. 10, p. 211–216.

Moore, J.C., 1989, Tectonics and hydrogeology of accretionary prisms: Role of the décollement zone: Journal of Structural Geology, v. 11, p. 95–106.

Moore, J.C., and Vrolijk, P., 1992, Fluids in accretionary prisms: Reviews of Geophysics, v. 30, p. 113–135.

Moore, J.C., Orange, D.L., and Kulm, L.D., 1990, Interrelationship of fluid venting and structural evolution: ALVIN observations from the frontal accretionary prism: Oregon: Journal of Geophysical Research, v. 95, p. 8795–8808.

Mottl, M.J., and Wheat, C.G., 1994, Hydrothermal circulation through mid-ocean ridge flanks: Fluxes of heat and magnesium: Geochimica et Cosmochimica Acta, v. 58, p. 2225–2237.

Muir Wood, R., 1994, Earthquakes, strain-cycling and the mobilization of fluids, *in* Parnell, J., ed., Geofluids: Origin, migration and evolution of fluids in sedimentary basins: Geological Society [London] Special Publication 78, p. 85–98.

Saffer, D.M., Silver, E.A., Fisher, A.T., Tobin, H., and Moran, K., 2000, Inferred pore pressures at the Costa Rica subduction zone: Implications for dewatering processes: Earth and Planetary Science Letters, v. 177, p. 193–207.

Shipley, T.H., McIntosh, K.D., Silver, E.A., and Stoffa, P.L., 1992, Three-dimensional imaging of the Costa Rica accretionary prism: Structural diversity in a small volume of the lower slope: Journal of Geophysical Research, v. 97, p. 4439–4459.

Sibson, R., 1994, Crustal stress, faulting and fluid flow, *in* Parnell, J., ed., Geofluids: Origin, migration and evolution of fluids in sedimentary basins: Geological Society [London] Special Publication 78, p. 69–84.

Stein, C., and Stein, S., 1994, Constraints on hydrothermal heat flux through the oceanic lithosphere from global heat flow: Journal of Geophysical Research, v. 90, p. 11,383–11,396.

Valentine, R., Morris, J.D., and Duncan, D., 1997, Sediment subduction, accretion, underplating, and arc volcanism along the margin of Costa Rica: Constraints from Ba, Zn, Ni, and ^{10}Be concentrations: Eos (Transactions, American Geophysical Union), v. 78, p. F673.

Yamano, M., and Uyeda, S., 1990, Heat flow studies in the Peru trench subduction zone, *in* Suess, E., et al., Proceedings of the Ocean Drilling Program, Scientific results, Volume 112: College Station, Texas, Ocean Drilling Program, p. 653–666.

Manuscript received December 1, 1999
Revised manuscript received May 2, 2000
Manuscript accepted May 10, 2000